Nanoscale

Accepted Manuscript

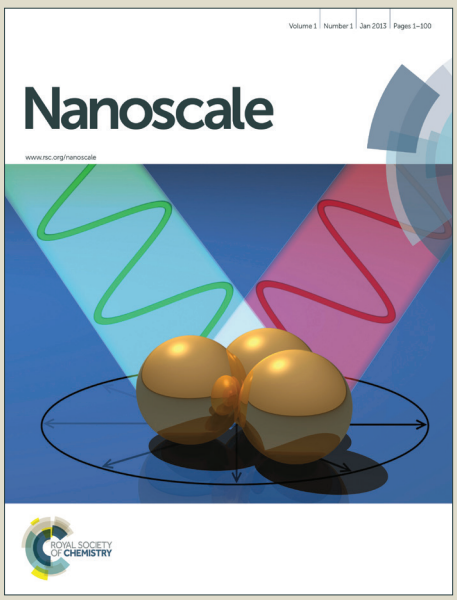

ROYAL SOCIETY OF CHEMISTRY

www.rsc.org/nanoscale

Cite this: DOI: 10.1039/c0xx00000x

www.rsc.org/xxxxxx

ARTICLE TYPE

Co_3O_4 Nanowires Supported on 3D N-Doped Carbon Foam as Electrochemical Sensing Platform for Efficient H_2O_2 Detection

Minmin Liu,[a,b] Shuijian He [a,b] and Wei Chen*[a]

Received (in XXX, XXX) Xth XXXXXXXXX 20XX, Accepted Xth XXXXXXXXX 20XX

DOI: 10.1039/b000000x

Using a simple hydrothermal procedure and the subsequent annealing treatment, one-dimensional (1D) cobalt oxide nanowires (Co_3O_4-NWs) with tunable size have been successfully *in situ* fabricated on three-dimensional (3D) carbon foam (CF) network. By changing hydrothermal treating time (0.5, 1, 2 h) at 180 °C, size-controlled Co_3O_4 nanowires can be formed on the CF. Scanning electron microscopy (SEM) and high-resolution transmission electron microscopy (HRTEM) measurements showed that nanoporous Co_3O_4 nanowires are uniformly grew on the 3D carbon framework. Due to the three-dimensional porous architecture and the high conductivity of the carbon foam skeleton, the obtained composites possess fast mass transport, large surface area and high electronic conductivity, which make them very promising as electrochemical sensing materials. Among the studied composites, the Co_3O_4-NWs/CF hydrothermally treated for 1 h exhibited the lowest detection limit (1.4 μM) and the largest linear ranges (0.01-1.4 mM) with a sensitivity of 230 nA μM^{-1} cm^{-2} for H_2O_2 detection. The present study shows that metal oxides supported on 3D carbon materials present a class of promising sensing platform for electrochemical detection of H_2O_2.

1. Introduction

Hydrogen peroxide (H_2O_2) has been widely used in many fields such as direct borohydride-hydrogen peroxide fuel cells, clinical studies, chemistry, biology, environmental protection, textile and food manufacturing *etc.* due to its high availability, easy storage, effortless handling and fast reduction kinetics than oxygen.[1-3] Up to now, a great variety of methods have been developed for H_2O_2 detection, such as titration, spectroscopy, chemiluminescence, electrochemical methods and so on. Among these methods, electrochemical technique is considered to be one of the efficient methods for H_2O_2 analysis because of its simple operation, high sensitivity and good selectivity. In electrochemical detections, oxidation or reduction of H_2O_2 at ordinary solid electrodes are limited by slow electrode kinetics and high overpotential which will cause the degradation of the sensing performance.[1] Therefore, electrocatalysts are the key components for H_2O_2 detection in electrochemical sensors. Many electrocatalysts have been reported for H_2O_2 reduction, such as mono- and bi-metallic nanoparticles (e.g. Ag, Au, PdPt, PdAg, *etc.*)[4-7] and transition-metal oxides (e.g. Fe_3O_4, Co_3O_4, Cu_2O, CuO) with different morphology and sizes.[8-10] However, metal or metal oxide catalysts usually suffer from dissolution and agglomeration during electrochemical processes, degrading the activities of catalysts and further the performances of electrochemical sensors.[11] To conquer the obstacles, nanostructured supports have been used to stabilize the electrocatalysts. Among various catalyst supports, three-dimensional carbon materials such as, 3D graphene foams,[11, 12] 3D carbon nanotubes (CNTs),[13] 3D CNT/graphene sandwiches,[14] mesoporous carbons[15, 16] have received increasing interests, due to their remarkable mechanical strength, outstanding electrical properties, and ultra-large surface area.

Recently, transition-metal oxides such as Co_3O_4, Fe_3O_4, SnO_2, MnO_2 etc. supported on carbon materials (graphene, CNTs) have been successfully synthesized and used as advanced materials for energy storage and conversion.[17, 18] Cobalt oxide (Co_3O_4) is a kind of intrinsic *p*-type semitransition metal oxide, exhibiting intriguing magnetic, electrochemical, gas sensing and electrocatalytic properties.[9, 19] Co_3O_4 with different morphologies such as nanospheres, nanocubes, nanofibers, and mesoporous structures have been successfully prepared by different synthetic routes.[20] In the present study, Co_3O_4 nanowires were synthesized via the combination of hydrothermal process and the subsequent annealing treatment. The morphology and the crystallization degree of Co_3O_4 nanowires can be controlled by the hydrothermal process and the annealing treatment.

Carbon foam (CF) obtained *via* thermal-treating commercially available melamine foam (MF) has 3D porous structure with extremely high porosity, which can offer large number of pores, ultra-large surface area with abundant active sites and fast mass transport.[21, 22] We report here for the first time Co_3O_4 nanowires supported on 3D nitrogen-doped carbon foam (CF) as electrochemical sensor for H_2O_2 detection. The 3D CF can offer conductive scaffolds to support the Co_3O_4 nanostructures and thus enhance the electrical conductivity of the overall electrode material, which is advantageous for electrochemical detection of H_2O_2. The electrochemical studies showed that the 3D Co_3O_4-

NWs/CF hybrids exhibit high sensitivity for H_2O_2 detection due to the following advantages of the 3D hierarchical structures. Firstly, microporous CFs have high stability and allow the easy diffusion of electrolyte onto the surface of the electro-active materials, accompanying reduced internal resistance. Secondly, the Co_3O_4 nanowires fabricated directly on the surface of carbon foams, preventing the tedious procedure of mixing active materials with binders.[23] Finally, the nanocrystallites on the Co_3O_4 nanowires can efficiently increase the surface area of the electrocatalysts, which could improve the utilization of the Co_3O_4 active material.[23] In addition, the possible growth mechanism of Co_3O_4 nanowires on CF was discussed. This study indicates that metal oxide nanomaterials supported on 3D carbon support represent a class of promising electrode material for electrochemical detection of hydrogen peroxide.

2. Experimental Section

2.1 Reagents and Materials

Melamine foam (MF) was supplied by Puyang Green Universh Chemical Co., Ltd. Cobalt nitrate hexahydrate ($Co(NO_3)_2$ $6H_2O$, A.R. grade, ≥ 99.0%), urea ($CO(NH_2)_2$, A.R. grade, ≥ 99.0%), potassium hydroxide (KOH, A.R. grade, ≥ 85.0%), glucose ($C_6H_{12}O_6$, A.R. grade, ≥ 99.0%), ascorbic acid (AA, $C_6H_8O_6$ A.R. grade, ≥ 99.7%), sodium chloride (NaCl, A.R. grade, ≥ 99.0%) and cetyltrimethylammonium bromide (CTAB, A.R. grade, ≥ 99.0%) are all purchased from Beijing Chemical Agent. Uric acid (UA, $C_5H_4N_4O_3$, ≥ 99.0%) was obtained from Wokai Chemical Limited (China). Dopamine (DA) and L-cysteine (Cys ≥ 98.0%) was purchased from Alfa. H_2O_2 solution (30 %) was purchased from Shanghai Lingfeng Chemical Reagent Co., Ltd, and the fresh H_2O_2 solutions with different concentration were prepared daily. All aqueous solutions were prepared with ultrapure water (18.3 MΩ cm). Ultrapure N_2 (≥ 99.999%) and Ar (≥ 99.999%) were supplied by the Changchun Juyang gas limited liability company.

2.2 Synthesis of Co_3O_4-NWs/CFs and unsupported Co_3O_4 NWs

Carbon foam (CF) was prepared by carbonizing MF under Ar flow of 100 mL min^{-1}. MF was first cut into pieces with the size of 0.5cm × 3cm × 20cm before carbonization. Carbonization process was as follows. First, the temperature was raised from room temperature to 300 °C at the rate of 5 °C min^{-1} and kept for 5 min. Second, the temperature was further raised to 400 °C at the rate of 1 °C min^{-1} and kept for 5 min. Finally, the temperature was raised to 700 °C at the rate of 2 °C min^{-1} and kept for 1 h. The carbonized carbon foams were further treated with 2.5 M nitric acid at 120 °C in 100 mL Teflon autoclave for 1 h to obtain oxygen-containing active sites. The synthesis of Co_3O_4/CF nanostructures were achieved by combining a simple hydrothermal treatment and a subsequent thermal annealing process.[24] Cobalt nitrate [$Co(NO_3)_2 \cdot 6H_2O$] was used as the cobalt precursor, and urea [$CO(NH_2)_2$] was used as the precipitant. In a typical synthesis, 0.45 g CTAB and 0.6 g urea were dissolved in 36 mL of 0.1 M $Co(NO_3)_2$ solution to form a homogeneous pink solution. The solution was then ultrasounded for 10 min to form a transparent solution. After that, three pieces of 45 mg carbon foams were immersed into the solution. The system was stirred gently overnight and divided into 3 partials and transferred into 20-mL Teflon autoclave for hydrothermal reaction at 180 °C for different times (0.5, 1 or 2 h, respectively). The synthesized samples for different reaction times are denoted as Co_3O_4-NWs/CF-0.5, Co_3O_4-NWs/CF-1 and Co_3O_4-NWs/CF-2, respectively. The products were washed with water and ethanol for several times to remove the excess surfactant and dissociative ions and then dried at 60 °C. The cobalt oxide species/CFs were annealed at 350 °C for 3 h under Ar gas with a heating rate of 5 °C min^{-1} to obtain crystalline cobalt oxide.

The unsupported Co_3O_4-NWs were synthesized by the same hydrothermal method at 180 °C for 1 h in the absence of carbon foam.

2.3 Materials Characterization

High-resolution transmission electron microscopy (HRTEM) measurements were performed on a JEM-2010(HR) microscope operated at 200 kV. The powder X ray diffraction (XRD) of the product was carried out on a PW1700 Powder diffractometer, using Cu Kα radiation with a Ni filter (λ=0.154059 nm at 30 kV and 15 mA) with scanning rate of 3 deg/min. Xray photoelectron spectroscopic (XPS) analysis was performed on a VG Thermo ESCALAB 250 (VG Scientific) operated at 120 W. The loadings of Co_3O_4 in the Co_3O_4/CF composites were measured by thermal gravimetric analysis (TGA) method using TA Instruments SDT Q600. In TGA measurement, the products were heated to 800 °C with a heating rate of 10 °C min^{-1} under air flow.

2.4 Electrochemical measurements

Electrochemical measurements were performed on a computer-controlled CHI 660 D electrochemical workstation to study the electrochemical activities of the synthesized Co_3O_4-NWs/CF composites for H_2O_2 reduction. Electrochemical measurements were carried out in a conventional three-electrode system fitted with a magnetic stirrer. The samples modified glassy carbon (GC) electrode was used as working electrode. A platinum coil (0.5 mm × 4 cm) and a Ag/AgCl (in saturated KCl, aq.) electrode were used as the auxiliary electrode and reference electrode, respectively. Before the deposition of the samples onto the GC electrode surface, a GC electrode (3.0 mm in diameter) was polished with 0.3 μm alumina slurries and cleansed by ultrasonication in 0.1 M HNO_3, 0.1 M H_2SO_4, and pure water, successively. The Co_3O_4-NWs/CF samples were crushed and dispersed in water with the concentration of 1 mg mL^{-1}. A 940 μL portion of the Co_3O_4-NWs/CF solution was mixed with 60 μL of 5 wt% Nafion solution by ultrasonication for a few seconds. Once the ink formed homogeneously, 4 μL of the ink was dropped on the clean surface of GC electrode and dried at room temperature.

3. Results and Discussion

3.1 Synthsis and characterization of Co_3O_4 nanowires supported on 3D carbon framworks

The morphologies and structures of the carbon foam (CF) and the Co_3O_4-NWs/CF composites prepared for different reaction time were first examined by SEM and TEM. As shown in Fig. 1a, the carbon foam shows a 3D porous structure with a smooth surface and thin carbon skeleton. The width of the carbon skeleton is

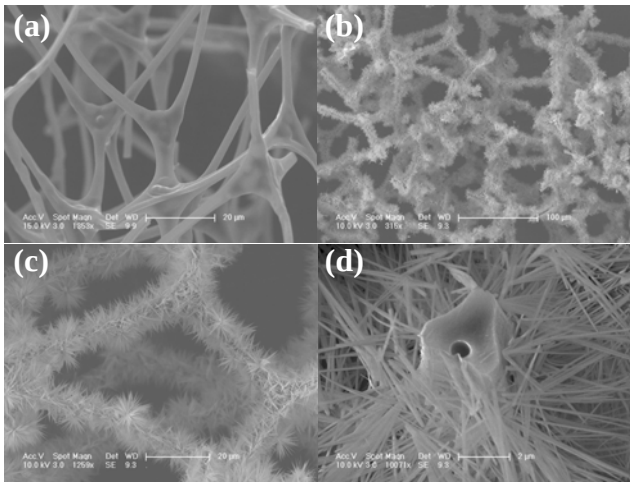

Fig. 1 (a) SEM image of carbon foam (CF). (b-d) SEM images of Co_3O_4 nanowires supported on CF (Co_3O_4-NWs/CF-1) at different magnifications.

about 100-120 μm. For the Co_3O_4-NWs/CF-1, it can be seen from the SEM images at different magnifications (Fig. 1b-d) that the skeleton of carbon foam is fully and uniformly covered by the as-grown Co_3O_4 nanowires with 100-200 nm in diameter and about 4.7-0.8 μm in length. However, we found that the time of hydrothermal treatment has significant effect on the morphology of the products. For the sample with the reaction time of 0.5 h (Co_3O_4-NWs/CF-0.5), only parts of the carbon foams are covered by Co_3O_4 nanowires and most of the carbon frameworks are naked and decorated by small nanocubes (Fig. S1), indicating 0.5 h is not enough for the full growth of Co_3O_4 nanowires. When reaction time increased to 2 h, the product (Co_3O_4-NWs/CF-2) shows blocky structure with very thick nanowires (Fig. S2). The bulky structure can not only largely reduce the surface area, but also lower the electro-conductibility and thus the electrochemical performance of the composite. Therefore, 1 h is the optimal reaction time for the formation of uniform Co_3O_4 nanowires on carbon foam. Interestingly, the HRTEM images shown in Fig. 2a-c indicate that the Co_3O_4 nanowires are actually porous and composed of small nanoparticles (10-20 nm in diameter). The intervals among the nanocrystals result in large accessible surface area and increased catalytically active sites, which is favorable for the full utilization of the Co_3O_4 nanowires.[9] From Fig. 2c, the nanoparticles exhibit high crystallinity with a fringe spacing of 0.288 nm, corresponding to the (220) planes of Co_3O_4.[19] The FFT patterns shown in the inset of Fig. 2c confirms the single crystallinity of the obtained Co_3O_4 nanowires.

The crystalline phase of the CFs-supported Co_3O_4 nanowires (Co_3O_4-NWs/CF-1) was investigated by X-ray diffraction (XRD) analysis. By comparing the XRD pattern of the sample and the standard data from the Joint Committee on Powder Diffraction Standards (JCPDS), all of the diffraction peaks can be indexed to Co_3O_4. (JCPDS card no. 42-1467).[25] The diffraction peaks observed at the 2θvalues of 19.1°, 31.3°, 36.9°, 44.8°, 59.6°, 65.4° are assigned to (111), (220), (311), (422), (511), (440) of Co_3O_4 phase (Fig. 2d).

To further elucidate the chemical composition of the as-grown

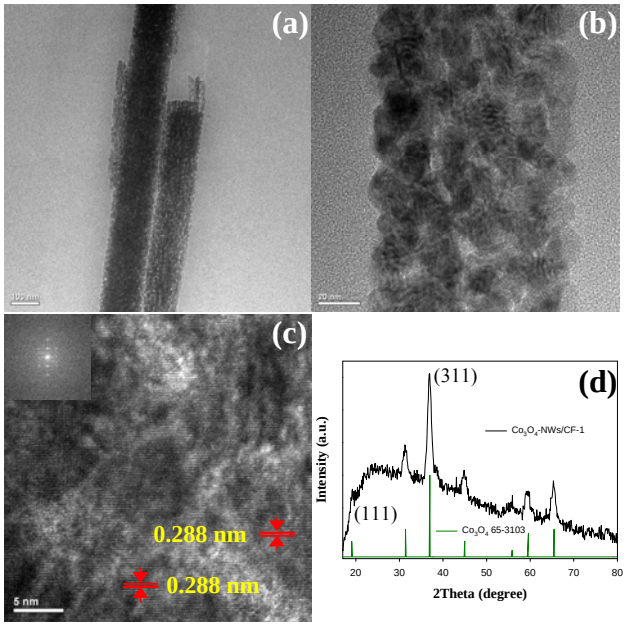

Fig. 2 (a-c) HRTEM images of the as-synthesized Co_3O_4 nanowires supported on CF (Co_3O_4-NWs/CF-1) at different magnifications. The inset in (c) shows the corresponding fast Fourier transform (FFT) pattern. (d) XRD pattern of the as-synthesized Co_3O_4-NWs/CF-1. For comparison, the XRD data of Co_3O_4 from the JCPDS (65-3103) were also included.

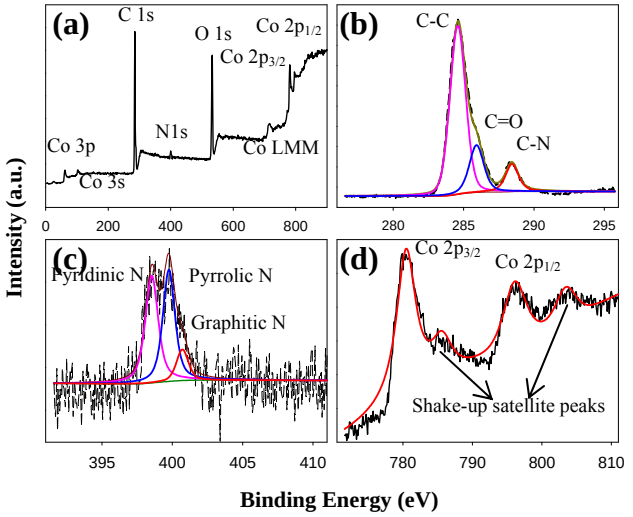

Fig. 3 (a) XPS survey spectrum of Co_3O_4-NWs/CF-1. (b-d) Deconvoluted high resolution XPS spectra of C 1s (b), N 1s (c) and Co 2p (d).

Co_3O_4-NW/CFs hybrids, X-ray photoelectron spectroscopy (XPS) measurements were carried out. In the XPS survey spectrum of the Co_3O_4-NWs/CF-1 (Fig. 3a), a series of sharp signals correspond to the characteristic peaks of C 1s, O 1s, N 1s, Co 3s, Co 3p, and Co 2p, indicating the existence of carbon, oxygen, nitrogen and cobalt elements in the prepared composites.[26] The high resolution C1s spectrum (Fig. 3b) can be devoluted into three peaks at 284.59, 285.95, and 288.44 eV, which are ascribed to C-C, C-N, and C=O, respectively. N 1s analysis (Fig. 3c) shows three different types of nitrogen atoms: pyridinic (398.54 eV), pyrrolic (399.76 eV), and graphitic (400.72 eV) N atoms.

Cite this: DOI: 10.1039/c0xx00000x

www.rsc.org/xxxxxx

ARTICLE TYPE

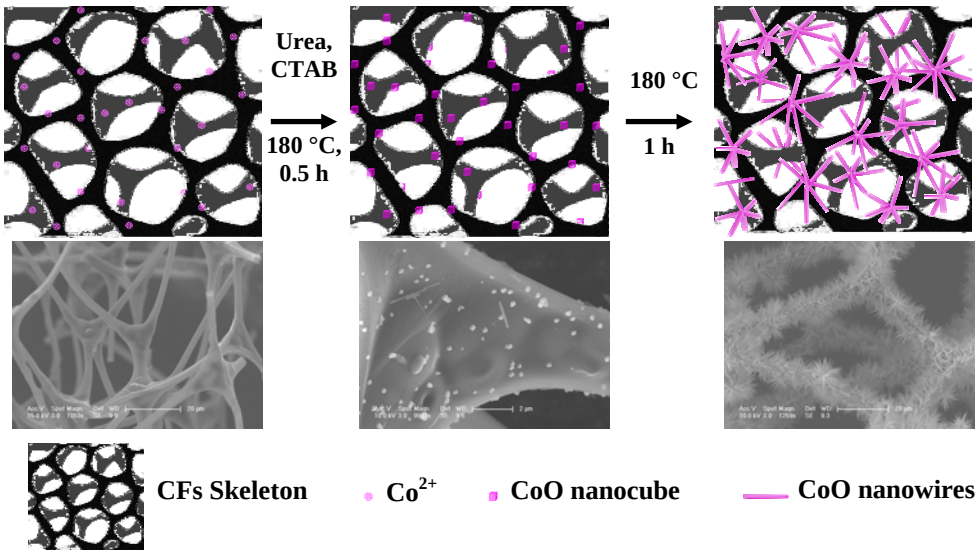

Scheme 1 Schematic illustration for the growth mechanism of Co_3O_4 nanowires on 3D carbon foams.

The previous experimental and theoretical studies[27, 28] showed that heteroatoms (N, S etc.) doping can enhance the electrocatalytic activities of carbon materials, especially for the oxygen reduction reaction (ORR). Here, the N-doping in the carbon foam support may enhance the catalytic activities of the Co_3O_4-NWs/CF hybrids and thus improve the H_2O_2 detection performance. In the Co 2p XPS spectrum (Fig. 3d), the two characteristic peaks centered at 780.6 and 796.2 eV correspond to Co 2p3/2 and Co 2p1/2 spin-orbit peaks of Co_3O_4 phase, respectively.[18, 26] Moreover, the two shake-up satellite peaks centered at 785.8 eV and 803.7 eV suggest the presence of Co^{2+} ions.[19, 29] The XPS results are in accordance with the color change of samples from original pink to black, suggesting the conversion of the samples from $Co(CO_3)_{0.5}OH$ to Co_3O_4 by the thermal treatment. Above SEM, TEM XRD and XPS measurements clearly indicate that Co_3O_4 nanowires have been formed on the carbon framework with the present synthetic routes. The 3D network of the carbon support and the porous structure of the Co_3O_4 nanowires render the hybrid materials promising electrochemical sensing platform with enhanced surface area, electron and mass transport.

The possible mechanism of the formation process of Co_3O_4 nanowires on the 3D carbon foam is shown in Scheme 1. The length of the Co_3O_4 nanowires can be simply tuned by adjusting the growth time as the proposed mechanism.[30] The formation of Co_3O_4 nanowires involves a hydrolysis-precipitation process, in which urea plays critical roles for the simultaneously hydrolysis-precipitation of bivalent Co^{2+} ions. The main reactions in the system can be expressed as follows:[31-33]

$H_2NCONH_2 + H_2O \rightarrow 2NH_3 + CO_2$ (1)

$CO_2 + H_2O \rightarrow CO_3^{2-} + 2H^+$ (2)

$NH_3 + H_2O \rightarrow NH_4^+ + OH^-$ (3)

At the elevated temperature of 180 °C, orthorhombic cobalt carbonate hydroxide phase is first formed. The reaction can be formulated as follows:

$Co^{2+} + OH^- + 1/2CO_3^{2-} + nH_2O \rightarrow Co(CO_3)_{0.5}OH \cdot nH_2O$ (4)

The subsequent formation of Co_3O_4 occurs as follows:

$6Co(CO_3)_{0.5}OH \rightarrow 2Co_3O_4 + 3H_2O + 2CO + CO_2$ (5)

Urea was used in the reaction system as precipitator to adjust pH due to its slow hydrolysis rate and controlled generation of OH ions, which can induce slow homogeneous precipitation process and crystal growth of the products.[25] As shown in Scheme 1, in the presence of CTAB, cubic nanocrystal seeds were first formed and Co_3O_4 nanowire can then grow from the nanocubes. From the SEM images shown in Fig. S1 the formation of cobalt hydroxide nanocubic species can be obviously observed on the surface of carbon foams at the beginning. With the excessive CTAB in the system and increasing hydrothermal time, the cobalt hydroxide nanocubes could grow into cobalt carbonate hydroxide nanowires along the [220] plane.[34]

TGA analysis was carried out to study the loading of Co_3O_4. The TGA curves of Co_3O_4 composites are represented in Fig. S3. The TGA results showed that the loading of Co_3O_4 increases with the increasing of heating time. The weight percentage of Co_3O_4 in Co_3O_4-NWs /CF-0.5, Co_3O_4-NWs /CF-1, and Co_3O_4-NWs /CF-2 are estimated to be ~45%, 61%, and 66%, respectively, which is accordant to the SEM results.

3.2 Electrochemical detection of hydrogen peroxide based on the Co_3O_4-NWs/CF platforms

To study the application of the Co_3O_4-NWs/CF nanocomposites in electrochemical sensors, here the detection of H_2O_2 in alkaline solution is studied by using the fabricated Co_3O_4-NWs/CF sensing platforms. The 3D structure of carbon foam, together with the supported Co_3O_4 nanowires provide a large accessible surface area. Meanwhile, the micron-grade porous carbon foams and the open spaces between Co_3O_4 nanowires allow the easy

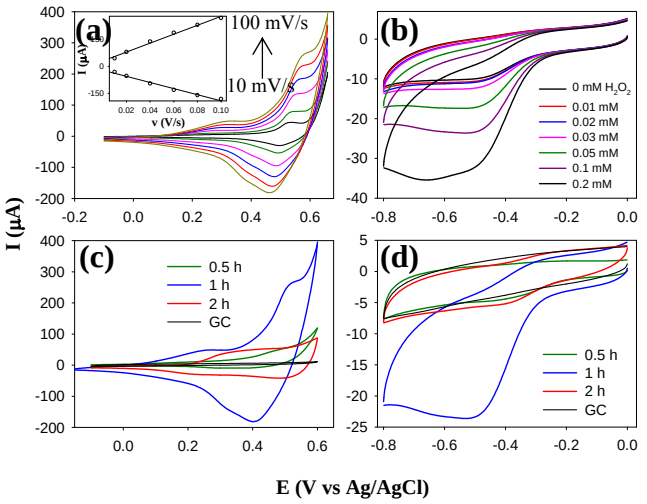

Fig. 4 (a) Cyclic voltammograms of Co_3O_4-NWs/CF-1 recorded in 0.1 M KOH solution at different potential scan rates from 10 to 100 mV s^{-1}. Inset: the dependence of oxidation and reduction peak currents on the potential scan rates. (b) Cyclic voltammograms of Co_3O_4-NWs/CF-1 in 0.1 M KOH solution with different concentrations of H_2O_2. (c) CV comparison of bare GC and the Co_3O_4-NWs/CFs composites in N_2-saturated 0.1 M KOH solution. (d) CV comparison of bare GC and the Co_3O_4-NWs/CFs in N_2-saturated 0.1 M KOH solution with the presence of 0.1 mM H_2O_2.

diffusion of electrolyte into the inter region of the electrode. Moreover, the cobalt oxide nanowires directly grown on the carbon foams have tight contacts with the carbon support, which make all the nanowires participate in the electrochemical detection and increase the sensing performance.[26] Since the structure and morphology of the Co_3O_4 nanowires are dependent on the hydrothermal reaction time (Fig. 1 and Fig. S1-2), the electrochemical properties of the three samples were firstly studied by cyclic voltammetry. Fig. 4a shows the cyclic voltammograms (CVs) of the Co_3O_4-NWs/CF-1 in N_2-saturated 0.1 M KOH solution at different potential scan rates. It can be seen that two redox current peaks can be observed within the potential range of 0-0.6 V (vs Ag/AgCl), which correspond to the following two redox processes:[34-37]

$$Co_3O_4 + OH^- + H_2O \Leftrightarrow 3CoOOH + e^- \quad (6)$$

$$CoOOH + OH^- \Leftrightarrow CoO_2 + H_2O + e^- \quad (7)$$

At different potential scan rates, the CV curves exhibit good symmetry, indicating the stable reversibility of the redox reaction of Co_3O_4 nanowires. Fig. 4a inset shows the dependence of oxidation and reduction peak currents on the potential scan rates. It can be seen that both anodic and cathodic peak currents increase linearly with the increase of scan rate, suggesting the surface-confined redox process. Meanwhile, the small shifts of the anodic and cathodic peak potentials with scan rates indicate the fast electron transfer kinetics of the 3D Co_3O_4-NWs/CF networks. The CV curves obtained from the Co_3O_4-NWs/CF-0.5 and Co_3O_4-NWs/CF-2 at different scan rates are shown in Fig. S4a and c. Similar CV features can be observed from the prepared materials. Fig. 4c compares the CVs of the three samples with the same mass loading. One can see that the largest redox currents were obtained from the Co_3O_4-NWs/CF-1. Such

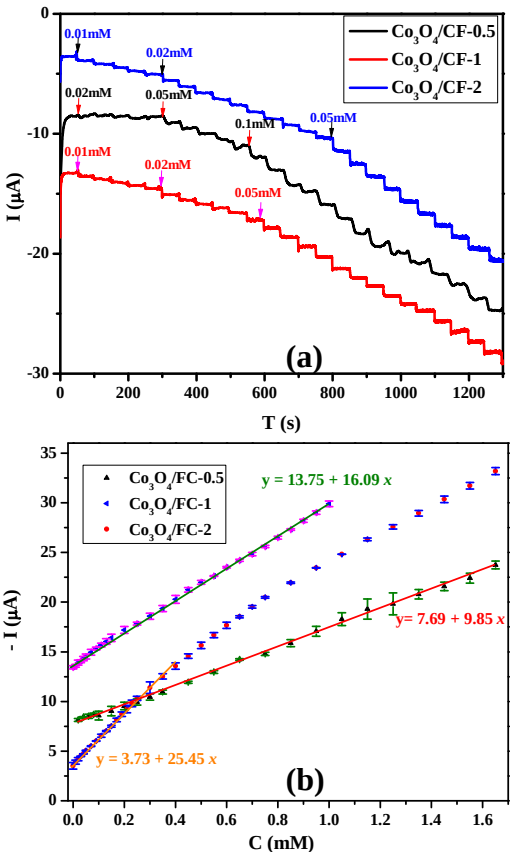

Fig. 5 (a) Amperometric response of Co_3O_4-NWs/CFs upon successive addition of H_2O_2 at the operating potential of -0.48 V (vs Ag/AgCl). (b) Corresponding calibration curves for the Co_3O_4-NWs/CFs towards H_2O_2 detection.

result agrees well with the above morphology characterizations. Compared to the uniform nanowires formed in the Co_3O_4-NWs/CF-1, the partially covered Co_3O_4 nanowires in the Co_3O_4-NWs/CF-0.5 and the bulk structure in the Co_3O_4-NWs/CF-2 result in lower electrochemical performance. For comparison, the CV obtained from bare GC electrode was also shown in Fig. 4c. It can be seen that compared to the large redox current from the Co_3O_4-NWs/CF composites, only much lower double-layer charging current was obtained from GC.

The electrochemical responses of the Co_3O_4-NWs/CF-1 to hydrogen peroxide reduction are shown in Fig. 4b. Compared to the CV in 0.1 M KOH with the absence of H_2O_2, an obvious reduction current can be observed upon the addition of H_2O_2 into the electrolyte and the current increases with increasing the H_2O_2 concentration. The CV curves of hydrogen peroxide reduction on Co_3O_4-NWs/CF-0.5 and Co_3O_4-NWs/CF-2 are shown in Fig. 4b and d. These voltammetric measurements indicate that the as-prepared Co_3O_4 nanowires have good electrocatalytic activities for H_2O_2 reduction. Fig. 4d shows the CVs of H_2O_2 reduction on bare GC and different Co_3O_4-NWs/CF samples with the same mass loading. At -0.48 V, the reduction current obtained from the Co_3O_4-NWs/CF-1 is approximately 3.3 times higher than those from other two electrodes, indicating the highest catalytic performance of Co_3O_4-NWs/CF-1 for H_2O_2 reduction. Due to the uniform and ordered Co_3O_4 nanowires, Co_3O_4-NWs/CF-1 shows

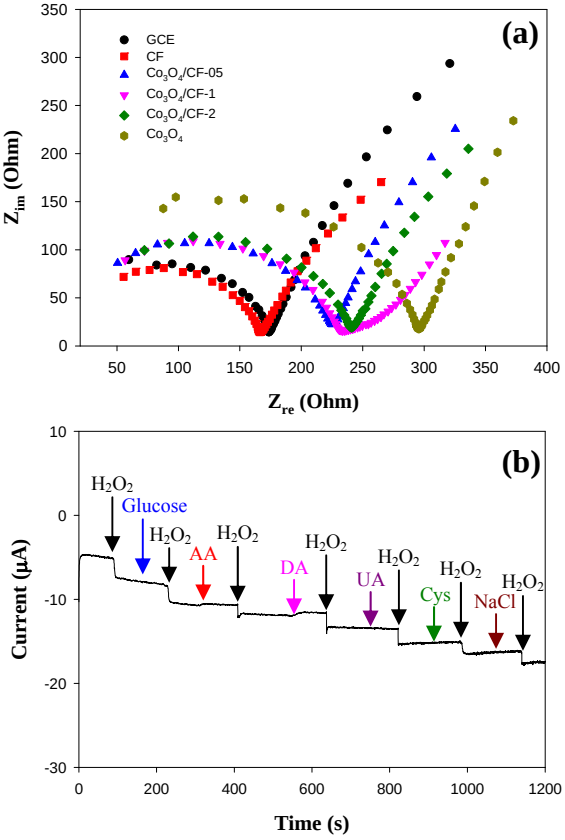

Fig. 6 (a) Electrochemical impedance plots of bare glassy carbon electrode (GCE), carbon foam (CF), three Co_3O_4-NWs/CF samples and Co_3O_4 in 0.1 M KOH. (b) The amperometic response of Co_3O_4-NWs/CF-1 to the addition H_2O_2 and other analytes in 0.1 M KOH at -0.48 V. The concentrations of the analytes are: 0.2 mM H_2O_2, 0.1 mM glucose, 0.1 mM ascorbic acid (AA), 0.1 mM dopamine (DA), 0.1 mM uric acid (UA), 0.1 mM L-cysteine (Cys), and 0.1 mM NaCl.

promising application in H_2O_2 electrochemical sensor.

At the holding potential of -0.48 V, the amperometric responses of the Co_3O_4/CF composite electrodes to successive addition of H_2O_2 were measured (Fig. 5a). The solution was kept stirring during the detection process to guarantee that H_2O_2 could be uniformly distributed in the electrolytic cell. It can be seen that the reduction current increases with increasing the concentration of H_2O_2, and the Co_3O_4/CF-1 and Co_3O_4/CF-2 have a fast response time (≤3 s), indicating a sensitive and rapid response to H_2O_2 reduction. However, the Co_3O_4-NWs/CF-0.5 exhibits a slow response time as long as 10 s, suggesting it is not an ideal candidate for H_2O_2 detection. The poor sensing performance of Co_3O_4-NWs/CF-0.5 might be attributed to the low coverage of Co_3O_4 nanowires on the carbon foam frameworks. Based on the reduction reaction of H_2O_2 on the Co_3O_4-NWs/CF materials, the mechanism of the electrochemical detection of H_2O_2 can be proposed as shown below:

$$CF/Co_3O_4 + H_2O_2 + e^- \rightarrow CF/Co_3O_4\text{-}OH_{ads} + OH^- \quad (8)$$

$$CF/Co_3O_4\text{-}OH_{ads} + e^- \rightarrow OH^- \quad (9)$$

$$2OH^- + 2H^+ \rightarrow 2H_2O \quad (10)$$

The corresponding calibration curves for H_2O_2 detection on the three sensing materials are plotted in Fig. 5b. In the present study, the limit of detection (LOD) of the Co_3O_4-NWs/CF-1 was calculated to be 1.4 μM (S/N > 3) in the linear H_2O_2 concentration range of 0.01-1.05 mM. Here, LOD = $3S_d/s$, s is the slope of the current-concentration curve and S_d is the standard deviation of any five current points without the presence of hydrogen peroxide in electrolyte. Such LOD is much lower than that of the Co_3O_4-NWs/CF-0.5 (85 μM) with a linear concentration range from 0.02 mM to 1.15 mM. As for the Co_3O_4-NWs/CF-2, although it shows the highest sensitivity for H_2O_2 detection at low concentration linear range, its LOD was calculated to be 4.5 μM with a narrow linear concentration range of 0.01-0.4 mM. Notably, the sensing performance of the present Co_3O_4-NWs/CF hybrids is remarkably higher than that of the Co_3O_4-based H_2O_2 sensors reported previously.[38, 39] The excellent electrochemical sensing performance of Co_3O_4-NWs/CF hybrids for H_2O_2 detection can be contributed to the 3D microporous structure of carbon foam, the full electrical connection of Co_3O_4 nanowires and carbon foam, and the open spaces between Co_3O_4 nanowires.[26] Detailedly, the 3D microporous carbon foam plays a role of supporting material. The Co_3O_4 nanowires directly grown on the carbon foams have tight contacts with the carbon support, which make all the nanowires participate in the electrochemical detection and increase the sensing performance.[23] The Co_3O_4 nanowires also can provide a large available surface area to enhance the electrochemical activities. Moreover, the open spaces between Co_3O_4 nanowires allow the easy diffusion of electrolyte into the inter region of the electrodes.

Electrochemical impedance spectroscopy (EIS) has been widely used as a forceful technique to study the interfacial electron-transfer properties of electrode materials.[40-42] As is known, the electron transfer resistance (R_{et}) can be reflected by the semicircle diameter in the Nyquist impedance plots. In an EIS measurement, a large semicircle means a high charge transfer resistance of the electrode, implying a low electron transfer rate. Fig. 6a shows the typical Nyquist plots of a bare GCE, carbon foam (CF), three Co_3O_4-NWs/CF samples and non-supported Co_3O_4 nanowires in 0.1 M KOH. The bare GCE holds a small semicircle diameter (black line) at high frequency, presenting a relative small R_{et}. The semicircle diameter has a little decrease with carbon foam modified onto the GCE (red line), indicating the extremely low R_{et} of the prepared carbon foam. For the GCE modified with non-supported Co_3O_4 nanowires (dark yellow line), the impedance largely increased, suggesting the high electron transfer resistance of cobalt oxide. However, when Co_3O_4 nanowires were supported on carbon foam (i.e. the prepared Co_3O_4-NWs/CF composites), the semicircle diameters decreased obviously. The EIS results clearly demonstrate that the carbon foam could largely enhance the electron transfer efficiency of the Co_3O_4-NW/CF hybrids.

To investigate the selectivity of the Co_3O_4-NWs/CF sensing platforms for H_2O_2 detection, the amperometic responses of Co_3O_4-NWs/CF-1 to H_2O_2 and other analytes, including glucose, ascorbic acid (AA), dopamine (DA) uric acid (UA), cysteine and NaCl, were studied. In the experiments, the concentration of H_2O_2 added into the detection system is 0.2 mM, while the concentration of each interfering species is 0.1 mM. As shown in

Fig. 6b, negligible current changes can be observed upon the addition of the interfering species. Such results indicate that the Co_3O_4-NWs/CF hybrids have great selectivity for H_2O_2 detection and have promising application as advanced H_2O_2 sensing materials.

4. Conclusions

In summary, a facile, environmentally friendly, and cost-efficient synthetic method was applied to the synthesis of Co_3O_4 nanowires supported on three dimensional carbon foams (Co_3O_4-NWs/CFs). With a hydrothermal reaction time of 1 h, a monolayer of uniform Co_3O_4 nanowires can be formed on the 3D carbon skeleton. The nanowires exhibit nanoporous structure with 200 nm in diameter and around 4.7 μm in length. The microporous carbon foam support and the nanoporous Co_3O_4 nanowires with enhanced specific surface area and electronic conductivity are very beneficial for their application as electrochemical sensing materials. The electrochemical measurements showed that the Co_3O_4-NWs/CF hydrothermally treated at 180 °C for 1 h (Co_3O_4-NWs/CF-1) exhibited the highest electrocatalytic activity towards H_2O_2 reduction. With the Co_3O_4-NWs/CF-1 as electrochemical sensing platform, hydrogen peroxide can be sensitively detected with good linear response ($R^2 = 0.9939$), low detection limit (1.4 μM) and a wide detection range (0.01-1.05 mM). However, the Co_3O_4-NWs/CFs with shorter (0.5 h) or longer (2 h) hydrothermal treatment time result in poorer sensing performance for H_2O_2 detection. The present study shows that Co_3O_4 nanowires in situ fabricated on 3D carbon support represent a type of novel electrochemical sensing platform for detection of H_2O_2.

Acknowledgements

This work was supported by the National Natural Science Foundation of China (No. 21275136) and the Natural Science Foundation of Jilin province, China (No. 201215090).

Notes and references

[a] *State Key Laboratory of Electroanalytical Chemistry, Changchun Institute of Applied Chemistry, Chinese Academy of Sciences, Changchun 130022, Jilin, China. Tel: +86431-85262061; E-mail: weichen@ciac.ac.cn*

[b] *University of Chinese Academy of Sciences, Beijing 100039, China*

† Electronic Supplementary Information (ESI) available: Additional TEM, TGA characterizations and electrochemical measurements of the as-prepared materials. See DOI: 10.1039/b000000x/

1. W. Chen, S. Cai, Q. Q. Ren, W. Wen and Y. D. Zhao, Analyst, 2012, 137, 49-58.
2. G. L. Wang, D. X. Cao, C. L. Yin, Y. Y. Gao, J. L. Yin and L. Cheng, Chem. Mater., 2009, 21, 5112-5118.
3. M. M. Liu, W. T. Wei, Y. Z. Lu, H. B. Wu and W. Chen, Chinese J. Anal. Chem., 2012, 40, 1477-1481.
4. T. C. Nagaiah, D. Schafer, W. Schuhmann and N. Dimcheva, Anal. Chem., 2013, 85, 7897-7903.
5. S. X. Mao, Y. M. Long, W. F. Li, Y. F. Tu and A. P. Deng, Biosens. Bioelectron., 2013, 48, 258-262.
6. B. Zhang, Y. L. Cui, H. F. Chen, B. Q. Liu, G. N. Chen and D. P. Tang, Electroanal., 2011, 23, 1821-1829.
7. Y. X. Fang, S. J. Guo, C. Z. Zhu, Y. M. Zhai and E. K. Wang, Langmuir, 2010, 26, 11277-11282.
8. S. M. Zhu, J. J. Guo, J. P. Dong, Z. W. Cui, T. Lu, C. L. Zhu, D. Zhang and J. Ma, Ultrason. Sonochem., 2013, 20, 872-880.
9. X. C. Dong, H. Xu, X. W. Wang, Y. X. Huang, M. B. Chan-Park, H. Zhang, L. H. Wang, W. Huang and P. Chen, Acs Nano, 2012, 6, 3206-3213.
10. M. M. Liu, R. Liu and W. Chen, Biosens. Bioelectron., 2013, 45, 206-212.
11. Z. S. Wu, S. B. Yang, Y. Sun, K. Parvez, X. L. Feng and K. Mullen, J. Am. Chem. Soc., 2012, 134, 9082-9085.
12. W. Wei, S. B. Yang, H. X. Zhou, I. Lieberwirth, X. L. Feng and K. Mullen, Adv. Mater., 2013, 25, 2909-2914.
13. W. Xiong, F. Du, Y. Liu, A. Perez, M. Supp, T. S. Ramakrishnan, L. M. Dai and L. Jiang, J. Am. Chem. Soc., 2010, 132, 15839-15841.
14. Z. J. Fan, J. Yan, L. J. Zhi, Q. Zhang, T. Wei, J. Feng, M. L. Zhang, W. Z. Qian and F. Wei, Adv. Mater., 2010, 22, 3723-3728.
15. D. S. Yang, D. Bhattacharjya, S. Inamdar, J. Park and J. S. Yu, J. Am. Chem. Soc., 2012, 134, 16127-16130.
16. R. Silva, D. Voiry, M. Chhowalla and T. Asefa, J. Am. Chem. Soc., 2013, 135, 7823-7826.
17. S. B. Yang, X. L. Feng, S. Ivanovici and K. Mullen, Angew. Chem. Int. Edit., 2010, 49, 8408-8411.
18. Z. S. Wu, W. C. Ren, L. Wen, L. B. Gao, J. P. Zhao, Z. P. Chen, G. M. Zhou, F. Li and H. M. Cheng, Acs Nano, 2010, 4, 3187-3194.
19. B. Varghese, T. C. Hoong, Z. Yanwu, M. V. Reddy, B. V. R. Chowdari, A. T. S. Wee, T. B. C. Vincent, C. T. Lim and C. H. Sow, Adv. Funct. Mater., 2007, 17, 1932-1939.
20. A. M. Cao, J. S. Hu, H. P. Liang, W. G. Song, L. J. Wan, X. L. He, X. G. Gao and S. H. Xia, J. Phys. Chem. B, 2006, 110, 15858-15863.
21. J. S. Lee, G. S. Park, S. T. Kim, M. L. Liu and J. Cho, Angew. Chem. Int. Edit., 2013, 52, 1026-1030.
22. S. L. Chen, G. H. He, H. Hu, S. Q. Jin, Y. Zhou, Y. Y. He, S. J. He, F. Zhao and H. Q. Hou, Energ. Environ. Sci., 2013, 6, 2435-2439.
23. R. B. Rakhi, W. Chen, D. Y. Cha and H. N. Alshareef, Nano Lett., 2012, 12, 2559-2567.
24. K. B. Xu, R. J. Zou, W. Y. Li, Y. F. Xue, G. S. Song, Q. Liu, X. J. Liu and J. Q. Hu, J. Mater. Chem. A, 2013, 1, 9107-9113.
25. S. K. Meher and G. R. Rao, J. Phys. Chem. C, 2011, 115, 25543-25556.
26. B. G. Choi, S. J. Chang, Y. B. Lee, J. S. Bae, H. J. Kim and Y. S. Huh, Nanoscale, 2012, 4, 5924-5930.
27. D. S. Geng, Y. Chen, Y. G. Chen, Y. L. Li, R. Y. Li, X. L. Sun, S. Y. Ye and S. Knights, Energ. Environ. Sci., 2011, 4, 760-764.
28. K. P. Gong, F. Du, Z. H. Xia, M. Durstock and L. M. Dai, Science, 2009, 323, 760-764.
29. Y. Wang, Z. Y. Zhong, Y. Chen, C. T. Ng and J. Y. Lin, Nano Res., 2011, 4, 695-704.
30. Q. Yang, Z. Y. Lu, Z. Chang, W. Zhu, J. Q. Sun, J. F. Liu, X. M. Sun and X. Duan, Rsc Adv., 2012, 2, 1663-1668.
31. Y. Wang, H. Xia, L. Lu and J. Y. Lin, Acs Nano, 2010, 4, 1425-1432.
32. S. L. Xiong, J. S. Chen, X. W. Lou and H. C. Zeng, Adv. Funct. Mater., 2012, 22, 861-871.
33. J. M. Ma and A. Manthiram, Rsc Adv., 2012, 2, 3187-3189.
34. Y. H. Xiao, S. J. Liu, F. Li, A. Q. Zhang, J. H. Zhao, S. M. Fang and D. Z. Jia, Adv. Funct. Mater., 2012, 22, 4052-4059.
35. Y. Y. Gao, S. L. Chen, D. X. Cao, G. L. Wang and J. L. Yin, J. Power Sources, 2010, 195, 1757-1760.
36. H. T. Wang, L. Zhang, X. H. Tan, C. M. B. Holt, B. Zahiri, B. C. Olsen and D. Mitlin, J. Phys. Chem. C, 2011, 115, 17599-17605.
37. Y. Y. Liang, H. L. Wang, P. Diao, W. Chang, G. S. Hong, Y. G. Li, M. Gong, L. M. Xie, J. G. Zhou, J. Wang, T. Z. Regier, F. Wei and H. J. Dai, J. Am. Chem. Soc., 2012, 134, 15849-15857.
38. W. Z. Jia, M. Guo, Z. Zheng, T. Yu, E. G. Rodriguez, Y. Wang and Y. Lei, J. Electroanal. Chem., 2009, 625, 27-32.
39. A. Salimi, R. Hallaj and S. Soltanian, Electroanal., 2009, 21, 2693-2700.
40. Y. Z. Lu and W. Chen, J. Phys. Chem. C, 2010, 114, 21190-21200.
41. Y. Z. Lu and W. Chen, Acs Catal., 2012, 2, 84-90.
42. Y. Han, J. B. Zheng and S. Y. Dong, Electrochim. Acta, 2013, 90, 35-43.